

---

*This document is the unedited Author's version of a Submitted Work that was subsequently accepted for publication in ACS Catalysis, copyright © American Chemical Society after peer review. To access the final edited and published work see <https://doi.org/10.1021/acscatal.8b04524>, see <http://pubs.acs.org/page/policy/articlesonrequest/index.html>.*

---

# Amine Transaminase from *Exophiala Xenobiotica* – Crystal Structure and Engineering of a Fold IV Transaminase that Naturally Converts Biaryl Ketones

*Aline Telzerow,<sup>a,b</sup> Juraj Paris,<sup>c,d</sup> Maria Håkansson,<sup>e</sup> Javier González-Sabín,<sup>d</sup> Nicolás Ríos-Lombardía,<sup>d</sup> Martin Schürmann,<sup>b</sup> Harald Gröger,<sup>c</sup> Francisco Morís,<sup>d</sup> Robert Kourist,<sup>a</sup> Helmut Schwab<sup>a</sup> and Kerstin Steiner<sup>a,\*</sup>*

[a] Institute of Molecular Biotechnology, Graz University of Technology, Petersgasse 14, 8010 Graz, Austria

[b] InnoSyn B. V. Urmonderbaan 22, 6167RD Geleen, The Netherlands

[c] Chair of Organic Chemistry I, Faculty of Chemistry, Bielefeld University, Universitätsstraße 25, 33615 Bielefeld, Germany

[d] Entrechem, S.L., Vivero Ciencias de la Salud, Santo Domingo de Guzmán, s/n, 33011 Oviedo, Spain

[e] SARomics Biostructures AB, Medicon Village, Scheelevägen 2, 22381 Lund, Sweden

**ABSTRACT:** Amine transaminases are frequently used for the production of chiral amines starting from prochiral ketones. These amines can be applied as active pharmaceutical ingredients or drug precursors. However, there are still limitations to the use of amine transaminases when it comes to bulky ketone substrates, such as biaryl ketones. Using data mining, an (*R*)-selective amine transaminase from *Exophiala xenobiotica* was identified which naturally converts biaryl ketone substrates to the corresponding amines with up to 85% conversion and excellent enantioselectivity (>99% *ee*). Its protein crystal structure was obtained with a resolution of 1.52 Å, which enabled us to explain this interesting substrate acceptance. Structure-guided protein engineering resulted in a quintuple variant with increased stability. Moreover, the amino acid exchange T273S increased the activity and broadened the substrate scope enabling conversions of various biaryl ketones with up to >99%. A preparative biotransformation of 1-(4-(pyridin-3-yl)phenyl)ethenone at 75 mM (15 g/L) resulted in 96% of isolated yield of the respective amine.

**KEYWORDS:** amine transaminase, biaryls, biosynthesis, enzyme catalysis, protein engineering

## INTRODUCTION

In the pharmaceutical industry, chiral amines play an important role as active pharmaceutical ingredients and as building blocks for drugs.<sup>[1]</sup> When these compounds are produced through biocatalysis, excellent enantioselectivity and therefore an enantiomeric excess of >99% *ee* as required for pharmaceuticals can be obtained. One class of enzymes that is used to produce chiral amines are amine transaminases (ATAs).<sup>[2]</sup> These enzymes reversibly catalyze the transfer of an amine group from an amino donor to a ketone or aldehyde. The co-factor pyridoxal 5'-phosphate (PLP) plays a crucial role by forming a Schiff base with the active site lysine of the enzyme.<sup>[3]</sup> PLP-dependent enzymes are classified according to their fold. ATAs belong to fold classes I and IV. In contrast to  $\alpha$ -amino acid aminotransferases, ATAs are not dependent on an  $\alpha$ -carboxylic acid moiety, therefore not limiting the product range to  $\alpha$ -amino acids.<sup>[4]</sup> Due to advanced protein engineering of existing biocatalysts or through novel enzyme discovery, the substrate scope of ATAs has been extended significantly, and several (*S*)-selective ATAs (fold-class I) have been engineered to convert a variety of sterically demanding ketones.<sup>[5]</sup> However, for (*R*)-selective ATAs (fold-class IV) the substrate spectrum is less versatile.<sup>[6]</sup> At the time, when our project started, only the engineered *Arthrobacter* ATA-117 from Codexis and Merck & Co, which was developed for Sitagliptin synthesis, was able to convert highly bulky ketones.<sup>[7]</sup> Particularly, the biaryl moiety has received increased attention as a privileged structure by the pharmaceutical industry, with examples of activity across a wide range of therapeutic substance classes including antifungal, anti-inflammatory, antirheumatic, antitumor, and antihypertensive agents.<sup>[8]</sup> The interest in this scaffold is further evident, as Bornscheuer and coworkers in parallel to us targeted the (*R*)-TA from *Aspergillus fumigatus* by protein engineering to make it suitable for the conversion of biaryl substrates.<sup>[9]</sup>

Our aim was to identify new (*R*)-selective ATAs that add to the existing toolbox of ATAs and expand the substrate scope within previously inaccessible bulky substrates. In this study we report the identification, characterization and enzyme engineering of an (*R*)-selective amine transaminase from *Exophiala xenobiotica* which naturally converts biaryl ketone substrates to the corresponding amines with up to 85% conversion and excellent enantioselectivity (>99% *ee*).

## MATERIAL AND METHODS

All chemicals were purchased from Sigma-Aldrich (St. Louis, MO, USA), Merck KGaA (Darmstadt, Germany) or Fluorochem (Hadfield, UK), if not stated otherwise. Materials for molecular biology were obtained from Thermo Fisher Scientific (Waltham, MA, USA), if not specifically mentioned.

### **Data Mining and Identification of a Suitable Amine Transaminase**

Published fold IV amine transaminase (ATA) sequences<sup>[7,10]</sup> were used to search for related sequences in the NCBI database (pBLAST).<sup>[11]</sup> The obtained protein sequences were aligned by Clustal $\omega$  with Mega6<sup>[12]</sup> and hits lacking the motif characteristic for fold IV ATAs<sup>[4]</sup> (Table S1) were excluded. The remaining sequences and their host organisms were screened for interesting features. The habitats of these organisms can for example give an indication on extremophilic environments resulting in particularly stable proteins or influencing the substrate scope of the enzymes. The transaminase (XP\_013320890) from *Exophiala xenobiotica* was chosen according to the origin of its host organism. The black yeast *E. xenobiotica* was isolated from environments that were associated with toxic, aromatic xenobiotics such as oil sludge, creosote-treated railway tie, soil polluted by gasoline or brown coal rich in phenolic compounds.<sup>[13]</sup> The hypothesis was that the presence and density of so many different aromatic compounds in the habitat of *E.*

*xenobiotica* might have led to a natural evolution of its amine transaminase to tolerate or accept these compounds.

### **Cloning and Mutagenesis**

The *E. xenobiotica* ATA gene was ordered codon-optimized for expression in *E. coli* from Geneart/LifeTech (Vienna, Austria). The gene was cloned via restriction digestion (*NdeI/HindIII*) and ligation (T4 ligase) into pMS470Δ8.<sup>[14]</sup> To add a C-terminal His-tag for purification, the transaminase gene of EX-ωTA was sub-cloned via PCR amplification and restriction digest (*NcoI/XhoI*) into the expression vector pET28a(+) from Novagen/Merck (Darmstadt, Germany). Desired mutations were introduced with PCR using primers with the desired mutation (Table S2) and the Phusion high fidelity polymerase.

### **Protein Expression and Purification**

After transformation of *E. coli* Top10F' cells (Invitrogen/LifeTechnologies, Carlsbad, CA, USA) with pMS470Δ8\_EX or *E. coli* BL21-Gold(DE3) (Stratagene, La Jolla, CA, USA) with pET28a(+)\_EX, the cells were grown at 37 °C in terrific broth medium supplemented with ampicillin (Amp: 100 μg mL<sup>-1</sup>) or kanamycin (Kan: 40 μg mg<sup>-1</sup>). Expression was induced with 0.1 mM Isopropyl β-D-1-thiogalactopyranoside (IPTG) at an OD<sub>600</sub> between 0.6-0.8 and carried out at 25 °C overnight. The cells were harvested at 4000 x g for 15 min and resuspended in buffer (pMS470Δ8 constructs: 50 mM KPi buffer, pH 7.5, 0.1 mM PLP; or pET28a(+) constructs: buffer A: 50 mM MES buffer, pH 6, 0.1 mM PLP, 50 mM NaCl, 10 mM imidazole). The cells were disrupted by sonication (Branson Sonifier S-250, 6 min, 80% duty cycle, 70% output) and centrifuged at 50000 x g for 1 h. The cleared lysates were filtered through 0.45 μm syringe filters. The protein concentration of the lysate was determined by Bradford protein assay. The expression and solubility of the proteins was analyzed by SDS-PAGE (NuPAGE Bis-Tris

PreCast Gels/Life Technologies). For purification of the His-tagged protein, the filtered cell-free lysate was incubated with Ni Sepharose™ 6 Fast Flow resin (GE Healthcare) for 20 min. The Ni Sepharose™ resin was then filled into empty PD-10 columns (GE Healthcare). After removal of impurities with buffer A containing 30 mM imidazole, the target protein was eluted with 300 mM imidazole in buffer A. Fractions were analyzed by SDS-PAGE, pooled, concentrated (Vivaspin 20 Centrifugal Filter Units; 10000 Da molecular weight cut-off; Sartorius, Göttingen, Germany) and desalted on PD-10 desalting columns (GE Healthcare) into 20 mM MES buffer pH 6 (containing 0.1 mM PLP, 50 mM NaCl). The concentration of the purified protein was determined with a Nanodrop spectrophotometer (model 2000c, Peqlab, Erlangen, Germany), using an absorbance of 1.43 at 280 nm, calculated based on the amino acid sequence using ProtParam.<sup>[15]</sup> The protein was frozen and stored at -20 °C until further use.

### **Crystallization and Structure Determination**

Screening for crystallization conditions was performed with a mosquito robot (TTP Labtech) using the screens JCSG+ and PACT *premier*™ (Molecular Dimensions) by the sitting drop vapor-diffusion method in MRC 3-well plates. A stock solution of purified EX- $\omega$ TA at 11 mg mL<sup>-1</sup> in 20 mM MES buffer pH 6 (containing 0.1 mM PLP, 50 mM NaCl) was used for all crystallization experiments. Drops of 400 nL were pipetted for screens with a 1:1 ratio of protein and screening solution. The crystallization plates were incubated in the dark at room temperature. Initial crystals of EX- $\omega$ TA were obtained at several crystallization conditions. A seed solution was made using seed beads (Hampton Research) and a mixture of initial crystals from several conditions of the JCSG+ screen stabilized in 100 mM SPG buffer, pH 8.5 and 25% (w/v) PEG1500. Seeding experiments were set up using 200 nL protein mixed with 30 nL seed and 170 nL reservoir. A new crystal form appeared in a condition containing 0.1 M sodium

acetate, pH 4.7 and 2 M ammonium sulfate. The crystal was transferred to a cryosolution containing 0.1 M sodium acetate (pH 4.6), 0.17 M ammonium sulfate, 25.5% w/v PEG1500, 15% v/v glycerol and flash-frozen in liquid nitrogen. Data collection was performed on the synchrotron beamline 14.1 (BESSY, Berlin, Germany) at 100 K. The data sets were processed and scaled using the XDS program package.<sup>[16]</sup> Molecular replacement was performed with Phaser<sup>[17]</sup> using the structure of the *Aspergillus terreus* ATA (PDB ID: 4CE5)<sup>[10e]</sup> as a search template. The resulting model was manually completed in Coot<sup>[18]</sup> and refined using Refmac5.<sup>[19]</sup> Data collection and processing statistics are summarized in Table S3. The final structure was checked using MolProbity.<sup>[20]</sup> The coordinates have been deposited in the protein data bank with accession code 6FTE. Since size exclusion chromatography suggested that the biological assembly of EX- $\omega$ TA is a dimer, which is in accordance with literature, the dimeric pdb file was generated with QtPISA.<sup>[21]</sup>

### **Substrate Docking and Visualization of Active Site Electrostatics**

Docking studies were performed with YASARA (version 18.4.24). To prepare the structure 6FTE for docking, the anisotropic temperature factors, any waters and other ligands were removed. The co-factor PLP was kept in the structure. After adding any missing hydrogens, the YASARA standard protocol for energy minimization was applied to the dimeric EX- $\omega$ TA structure. Structures of the substrates were drawn with ChemDraw (version 17.0.0.206(121)) and the energy was minimized with YASARA. A simulation cell was created around one active site of the dimeric structure of EX- $\omega$ TA and VINA docking was performed with the standard mcr\_dock with 999 runs. The docking result was chosen according to the best energy but also manual visualization and realistic positioning of the substrate.

For the visualization of the active site charge, PDB structures were loaded into PyMOL (version 2.1.1). The active site charge was calculated with the APBS electrostatics plugin for PyMOL and visualized accordingly.

### **Spectrophotometric Activity Assay**

The activity of the ATA variants was determined with an adjusted standard photometric assay.<sup>[22]</sup> Here, the substrate phenylethylamine is converted to acetophenone, which can be detected spectrophotometrically at 300 nm. The absorbance increases with rising product concentration. To measure the activities of the ATA variants, reactions were set up in 1 mL volume with 100 mM KPi buffer pH 7.5 containing 0.1 mM PLP, 5 mM phenylethylamine and 5 mM pyruvic acid. For the reaction, 50  $\mu$ g to 250  $\mu$ g of total protein were used. The production of acetophenone was measured for several minutes at 300 nm at 30 °C. The volumetric activity in U mL<sup>-1</sup> and the specific activity in U mg<sup>-1</sup> total protein of the enzyme samples was calculated using the Beer-Lambert law with the molar extinction coefficient of acetophenone  $\epsilon_{300} = 0.28 \text{ cm}^2 \mu\text{mol}^{-1}$ .

### **Biotransformations**

#### *Enzymes*

LDH (Lactate dehydrogenase) from rabbit muscle (Sigma-Aldrich, Type II, ammonium sulfate suspension, 800-1, 200 U mg<sup>-1</sup> protein).

GDH (Glucose dehydrogenase) from *Bacillus megaterium* was expressed in *Escherichia coli*.

The activity was determined as 1884 U mL<sup>-1</sup> according to the assay described in literature.<sup>[23]</sup>

EX- $\omega$ TA (amine transaminase from *Exophiala xenobiotica*) and its variants were expressed in *Escherichia coli*. The activity was measured spectrophotometrically (see above) and yielded:

EX-wt: 16.9 U mL<sup>-1</sup> or 4.5 U mg<sup>-1</sup> total protein, EX-X5: 37.7 U mL<sup>-1</sup> or 4 U mg<sup>-1</sup> total protein,



EX-STA: 23.35 U mL<sup>-1</sup> or 4.6 U mg<sup>-1</sup> total protein and EX-STA5: 23.35 U mL<sup>-1</sup> or 1.9 U mg<sup>-1</sup> total protein.

The (*S*)-alcohol dehydrogenase from *Rhodococcus ruber* DSM 44541 was provided as a cell-free extract (CFE) by InnoSyn B.V. (Geleen, The Netherlands).<sup>[24]</sup> The total protein concentration was about 46 mg mL<sup>-1</sup> with a good expression level of the ADH in the soluble fraction. The activity was determined spectrophotometrically at pH 6.0 with acetone and NADH as substrates and was 225 U mL<sup>-1</sup> or 4.85 U mg<sup>-1</sup> total protein, respectively.

### *Reagents*

1-(Biphenyl-4-yl)ethanone (**1a**) was purchased from Merck Schuchardt. Biaryl ketones (**1b-j**) were prepared as described in the literature.<sup>[25]</sup> D-(+)-Glucose was purchased from VWR. D-Alanine, PLP (Pyridoxal 5'-phosphate hydrate) and NAD<sup>+</sup> were purchased from Sigma Aldrich.

### *General methods*

<sup>1</sup>H-NMR and proton-decoupled <sup>13</sup>C-NMR spectra (CDCl<sub>3</sub>) were obtained using a Bruker DPX-300 (<sup>1</sup>H, 300.13 MHz and <sup>13</sup>C, 75.5 MHz) spectrometer using the δ scale (ppm) for chemical shifts. Calibration was made on the signal of the solvent (<sup>13</sup>C: CDCl<sub>3</sub>, 77.16; <sup>1</sup>H: CDCl<sub>3</sub>, 7.26).<sup>[26]</sup> High resolution mass spectra were recorded on a Bruker Impact II instrument. Optical rotations were measured using a Perkin-Elmer 241 polarimeter and are quoted in units of 10<sup>-1</sup> deg cm<sup>2</sup> g<sup>-1</sup>. HPLC analyses to determine the degree of conversion were carried out in an Agilent RR1200 HPLC system, using a reversed phase column (Zorbax Eclipse XDB-C18, RR, 18 μm, 4.6 x 50 mm, Agilent). HPLC analyses to determine *ee* values were performed on a Hewlett Packard 1100 LC liquid chromatograph. Details of HPLC methods and analyses including chromatograms can be found in the supporting information.

*General Procedure for the Screening of Ketones **1a-r** using EX- $\omega$ TA (Wild Type and Variants) and Alanine as Amino Donor*

The ketone (20 mM) was first dissolved in DMSO (32  $\mu$ L, 5% v/v) in a 2 mL reaction tube (Eppendorf). Then EX- $\omega$ TA lysate (**1a-j**: 8 U, **1k-r**: 20 U), potassium phosphate buffer (KPi) 100 mM pH 7.5, 1 mM PLP, 0.1 mM NAD<sup>+</sup>, D-glucose (57 mM), D-alanine (130 mM), LDH (90 U) and GDH (30 U) were added. The reaction was shaken at 30 °C and 250 rpm for 24 h. To determine the conversion, 10  $\mu$ L of the mixture were diluted with 90  $\mu$ L of DMSO and analyzed by achiral reverse phase with previous centrifuging and filtering of the sample. To determine the enantiomeric excess for reactions employing the ketones **1a-j**, the reaction was quenched by addition of aqueous 10 N NaOH (400  $\mu$ L). The mixture was then extracted with ethyl acetate (2  $\times$  500  $\mu$ L) and the organic layers were separated by centrifugation (90 s, 13000 rpm), combined and dried over anhydrous Na<sub>2</sub>SO<sub>4</sub>. The enantiomeric excess of amines was measured by chiral HPLC.

*General Procedure for the Screening of Biaryl Ketones **1a-j** using EX-STA and Isopropylamine as Amino Donor*

In a 2 mL reaction tube, ketone (20 mM) was first dissolved in DMSO (32  $\mu$ L, 5% v/v) and then ATA lysate (8 U), KPi buffer 100 mM pH 7.5, 1 M isopropylamine and 1 mM PLP were added. The reaction was shaken at 30 °C and 250 rpm for 24 h. To determine the conversion, 10  $\mu$ L of the mixture were diluted with 90  $\mu$ L DMSO and analyzed by achiral reverse phase with previous centrifuging and filtering of the sample. To determine the enantiomeric excess the reaction was quenched by addition of aqueous 10 N NaOH (400  $\mu$ L). The mixture was then extracted with ethyl acetate (2  $\times$  500 $\mu$ L) and the organic layers were separated by centrifugation (90 s, 13000 rpm), combined and dried over anhydrous Na<sub>2</sub>SO<sub>4</sub>. The enantiomeric excess of amines was measured by chiral HPLC.

*General Procedure for the Synthesis of Racemic Amine Standards 2a-g*

Ammonium formate (300 mg) and zinc (150 mg) were added to a solution of 80 mg ketone (**1a-g**) in 1.5 mL of ethanol and the mixture was stirred overnight at 80 °C under nitrogen. Then, the reaction mixture was cooled at room temperature, filtered through Celite and washed with ethanol. The solvent was removed under vacuum to obtain an oily crude, followed by the addition of 10 mL of aqueous 1 N HCl and washing with diethyl ether (2 × 20 mL). The aqueous layer was basified to pH 10 with aqueous 10 N NaOH and extracted with ethyl acetate (3 × 5 mL). The organic layer was washed with 10 mL of brine and dried over anhydrous Na<sub>2</sub>SO<sub>4</sub>. Further concentration on a rotary evaporator afforded the corresponding biaryl amine **2a-g** (25-30% yield).

*General Procedure for the Synthesis of Racemic Amine Standards 2h-j*

Et<sub>3</sub>N (2 eq) and MsCl (2 eq) were added to a solution of 80 mg alcohol (beforehand obtained by reducing the corresponding ketone with NaBH<sub>4</sub>) in 3.0 mL of dichloromethane and the mixture was stirred overnight at room temperature. Then, the solvent was removed and NaN<sub>3</sub> (10 eq) and anhydrous DMF (3 mL) were added, the resulting mixture being stirred at 70 °C for 24 h. Further evaporation of the solvent under reduced pressure afforded a crude which was purified by flash chromatography (EtOAc/hexane mixtures). Finally, to a suspension of the previous azido compound and Pd-C 10% (25 mg) in a round-bottom flask, a H<sub>2</sub> balloon was connected and deoxygenated MeOH (1.5 mL) carefully added. The resulting mixture was stirred at room temperature for 24 h. After this time, the mixture was filtered through Celite<sup>®</sup> and the solvent evaporated under reduced pressure to afford the corresponding biaryl amine **2h-j** (yield: 70-75%).

*General Procedure for the Synthesis of Enantiopure Biaryl Amine Standards*

In a 15 mL reaction tube, ketone (0.25 mmol) and ADH from *R. ruber* (16 U) were added to a *i*-PrOH (5 mL)/50 mM KPi buffer pH 7.0 (5 mL) mixture (1 mM NAD<sup>+</sup>). The reaction was shaken at 30 °C and 250 rpm for 24 h. The mixture was extracted with ethyl acetate (2 × 10 mL), the organic layers combined, dried over anhydrous Na<sub>2</sub>SO<sub>4</sub>, filtered and concentrated under vacuum to provide the corresponding (*S*)-alcohol (*ee* >99%).

Then, the corresponding (*S*)-alcohol (0.25 mmol) and diphenyl phosphoryl azide (DPPA, 0.30 mmol) were dissolved in dry toluene (0.4 mL). The mixture was cooled to 0 °C under N<sub>2</sub>, and DBU (0.30 mmol) was added. The reaction was stirred for 2 h at 0 °C and then at 20 °C for 16 h. The resulting mixture was washed with H<sub>2</sub>O (2 × 5 mL) and aqueous 1N HCl (5 mL). The organic layer was concentrated under reduced pressure and purified by flash chromatography (EtOAc/hexane mixtures). Finally, to a suspension containing the resulting azide compound and Pd-C 10% (10 mg) in a 25 mL round-bottom flask a H<sub>2</sub> balloon was connected and deoxygenated MeOH (1.0 mL) carefully added. The resulting suspension was stirred at room temperature for 24 h. After this time, the reaction mixture was filtered through Celite<sup>®</sup> and the solvent evaporated under reduced pressure to afford the corresponding (*R*)-biaryl amine as a colorless oil (*ee* = 97%, yield = 50-70%).

#### *Preparative-scale Transamination of **1i** using Lyophilized EX-STA*

After dissolving **1i** (75 mM, 100 mg) in DMSO (319 μL, 5% v/v) in a 50 mL reaction tube, lyophilized EX-STA (320 U, 700 mg), 100 mM KPi buffer pH 7.5 (5.8 mL, 1 mM PLP, 0.1 mM NAD<sup>+</sup>), D-glucose (114 mM, 293 mg), D-alanine (260 mM, 332 mg), LDH (3604 U, 682 μL) and GDH (1201 U, 400 mg) were added. The reaction was shaken at 30 °C and 250 rpm for 24 h. The reaction was quenched by addition of aqueous 10 N NaOH (10 mL) to adjust the pH to 14. The mixture was then extracted with ethyl acetate (2 × 20 mL) and the organic layers were separated

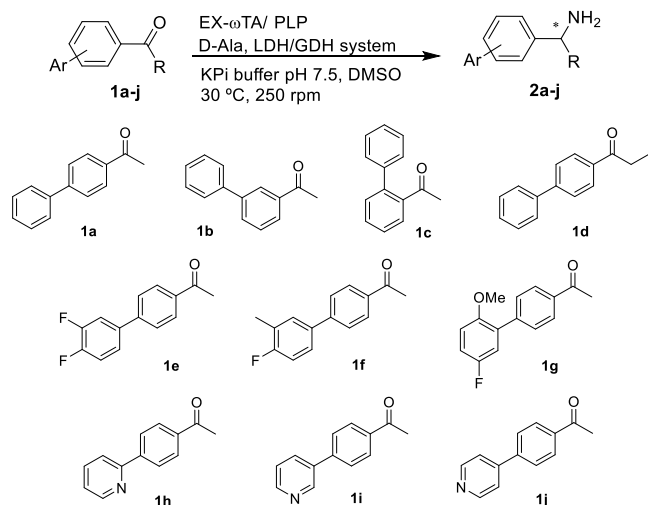
by centrifugation (90 s, 13000 rpm), combined and dried over anhydrous Na<sub>2</sub>SO<sub>4</sub>. Further evaporation under reduced pressure provided (*R*)-**2i** as a white solid in 96% yield (*ee* >99%).

## RESULTS AND DISCUSSION

To identify new (*R*)-selective ATAs that expand the substrate scope within previously inaccessible bulky substrates several sequences from literature were used for sequence-based similarity searches against the NCBI database.<sup>[7,10]</sup> (*R*)-amine transaminases are members of the fold type IV PLP-dependent enzyme family.<sup>[7,10]</sup> This family includes D-amino acid aminotransferases, L-branched chain aminotransferases and 4-amino-4-deoxychorismate lyases. In an analysis of fold class IV enzymes Bornscheuer and his group showed that amino acids in the active site, which are important for substrate binding, are conserved. Thus, they proposed motifs that can be used for the prediction of subgroups within this fold class (Table S1).<sup>[4]</sup> Sequences that lacked the motif characteristic for ATAs<sup>[4]</sup> were removed from the pool.

### **EX- $\omega$ TA converts biaryllic ketones**

*Exophiala xenobiotica*-ATA (EX- $\omega$ TA) was chosen based on the habitat of its host organism. The black yeast *E. xenobiotica* was isolated from environments that were associated with toxic, aromatic xenobiotics such as oil sludge, creosote-treated railway tie, soil polluted by gasoline or brown coal rich in phenolic compounds.<sup>[13]</sup> The hypothesis was that the presence and density of so many different aromatic compounds in the habitat of *E. xenobiotica* might have led to a natural evolution of its transaminase to accept some substrates that other ATAs do not tolerate. With these premises, the bioamination of 4'-phenylacetophenone (**1a**) catalyzed by EX- $\omega$ TA (Scheme 1) was investigated as a benchmark reaction.



**Scheme 1.** Amine transaminase-catalyzed transamination of biaryl ketones **1a-j** employing EX- $\omega$ TA.

Initially, the reaction was tested under the simplest reaction conditions, namely using isopropylamine (IPA) as amino donor. Indeed, this reagent is the preferred amino donor in industry due to its low cost and easy removal of the by-product acetone to shift the equilibrium.<sup>[27]</sup> However, despite testing excess of IPA at several donor-acceptor ratios in a broad pH range, no conversion was detected in any case. In fact, many wild-type ATAs are reluctant to accept IPA and this problem is only overcome after protein engineering. Thus, subsequently alanine was used as amino donor combined with the LDH/GDH system to shift the equilibrium. After thorough parametrization encompassing not only the involved enzymes and cofactors but also pH, amino donor and co-solvent, the enzymatic system worked efficiently according to the following reaction setup: **1a** (20 mM) in 100 mM phosphate buffer pH 7.5, supplemented with PLP (1 mM), NAD<sup>+</sup> (0.1 mM), glucose (60 mM), D-alanine (6.5-fold) and DMSO (5% v/v). 8 U of EX- $\omega$ TA were used (Scheme 1). After 24 h of incubation at 30 °C and 250 rpm, the corresponding biaryl amine (*R*)-**2a** was produced enantiomerically pure (>99% *ee*, Table 1, entry 1) with a conversion of 83%.

**Table 1.** Substrate scope of EX- $\omega$ TA and its variants. EX-STA variant represents amino acid exchange in the small binding pocket. EX-5 was engineered for improved stability. The variant EX-STA5 inherits the combined amino acid exchanges of EX-STA and EX-5.<sup>[a]</sup>

Entry	Substrate	EX-wt	EX-STA	EX-5	EX-STA5	<i>ee</i> (%) <sup>[b]</sup>
1	<b>1a</b>	83	45	15	45	>99 ( <i>R</i> )
2	<b>1b</b>	38	85	28	85	>99 ( <i>R</i> )
3	<b>1c</b>	-	-	-	-	n.d. <sup>[c]</sup>
4	<b>1d</b>	-	-	-	-	n.d. <sup>[c]</sup>
5	<b>1e</b>	25	72	84	55	>99 ( <i>R</i> )
6	<b>1f</b>	21	40	30	30	>99 ( <i>R</i> )
7	<b>1g</b>	25	30	30	24	>99 ( <i>R</i> )
8	<b>1h</b>	72	>99	40	80	>99 ( <i>R</i> )
9	<b>1i</b>	82	>99	50	95	>99 ( <i>R</i> )
10	<b>1j</b>	85	>99	82	70	>99 ( <i>R</i> )

[a] Reaction conditions: 20 mM ketone dissolved in DMSO (5% v/v), 100 mM potassium phosphate buffer, pH 7.5, 1 mM PLP, 0.1 mM NAD<sup>+</sup>, cell free *E. coli* lysate containing 8 U ATA (according to a spectrophotometric assay at 30°C in 100 mM potassium phosphate buffer, pH 7.5, 0.1 mM PLP, 5 mM phenylethylamine and 5 mM pyruvic acid as substrates), 130 mM D-alanine, 60 mM glucose, 30 U GDH and 90 U LDH, shaken for 24 h at 250 rpm and 30 °C. Conversions were measured by HPLC. [b] Measured by chiral HPLC; the *ee* is the same for all four enzymes. [c] Not detected due to low activity.

Encouraged by this result, the substrate scope of EX- $\omega$ TA was explored employing a panel of *ortho*-, *meta*-, *para*-biaryl and arylpyridine ketones, some of them exhibiting different patterns of substitution at the phenyl moiety next to the carbonyl group (Table 1, entries 2-10). While the

enzyme showed no detectable catalysis toward the *ortho*-biaryl ketone **1c** (Table 1, entry 3), a remarkable activity was observed for *meta*- and *para*-biaryl ketones. In particular, the unsubstituted arylpyridine ketones **1h-j** rendered conversions higher than 70% (Table 1, entries 8-10). The non-conversion toward 4'-phenylpropiophenone (**1d**) unveiled the size restrictions of EX- $\omega$ TA in the small binding pocket, which cannot accommodate substituents larger than a methyl group. Fluorine atoms on different positions on the aromatic ring in ketones **1e-g** had a negative impact on the conversion which was attributed to the strong electron-withdrawing effect of fluorine (Table 1, entries 5-7). It is worth noting that EX- $\omega$ TA displayed excellent asymmetric induction in the reductive amination of the carbonyl group of all the ketones, leading to the (*R*)-enantiomer of each amine with >99% *ee*.

### Structural characterization of EX- $\omega$ TA

For a better understanding of this unique substrate acceptance, the crystal structure of EX- $\omega$ TA was determined by X-ray crystallography at a resolution of 1.52 Å (PDB ID: 6FTE, Figure 1A, Table S3). The asymmetric unit contains one polypeptide chain. Size exclusion chromatography suggested that the biological assembly of EX- $\omega$ TA is a dimer, which is in accordance with literature.<sup>[10]</sup> The homo-dimeric structure of EX- $\omega$ TA showed the typical fold IV with the active site at the interface of the monomers and the co-factor PLP bound to the active site lysine 179 (Figure 1B). The electron density in the active site was well defined where the PLP was expected to bind (Figure S1). Moreover, additional density corresponding to a putative glycerol molecule was observed in the active site. EX- $\omega$ TA also contains an N-terminal  $\alpha$ -helix typical for (*R*)-selective amine transaminases<sup>[10]</sup>, which is not observed in any of the other fold IV subfamilies. A structural similarity search using the DALI server<sup>[28]</sup> confirmed that the closest homologous structures are indeed (*R*)-selective transaminases (PDB-code: 4CE5 from *Aspergillus terreus*<sup>[10e]</sup>,



Z-score: 51.1, rmsd 0.7 Å, seq id: 75%; PDB-code: 4CMD from *Nectria haematococca*<sup>[10b]</sup>, Z-score: 50.6, rmsd 0.7 Å, seq id: 74%; PDB-code: 4CHI from *Aspergillus fumigatus*<sup>[10a]</sup>, Z-score: 50.2, rmsd 0.8 Å, seq id: 70%; PDB-code: 3WWH from *Arthrobacter sp.* KNK168<sup>[10f]</sup>, Z-score: 41.8, rmsd 1.8 Å, seq id: 44%).

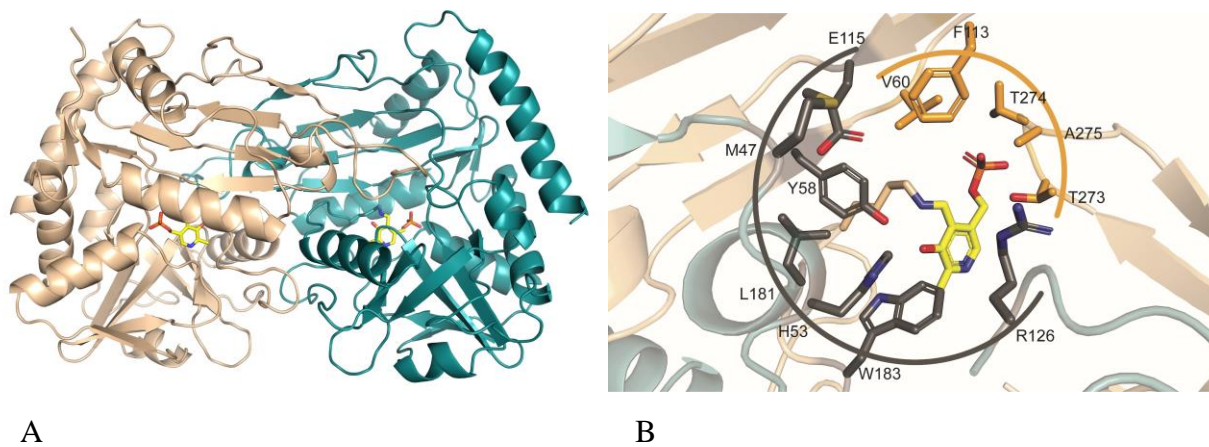


**Figure 1.** Crystal structure of EX- $\omega$ TA. A: Overview of the EX- $\omega$ TA dimer (chain A in orange, chain B in turquoise), PLP is indicated in yellow, B: Overview of the EX- $\omega$ TA dimer active site with the small binding pocket amino acids depicted in orange and the large binding pocket amino acids in dark grey. The figures were prepared using the program PyMOL.

The active site showed a comparable size to the ones from other fold IV ATAs<sup>[10a-b, 10e]</sup> and consisted of a small and a large binding pocket (Figure 1B). In general, the larger pocket accommodates the bulky substituent of the ketone substrate or the  $\alpha$ -amine of the co-substrate. The small binding pocket harbors the smaller substituent, usually a methyl-group.<sup>[4,10]</sup> As we could not obtain structure-ligand complexes by co-crystallization nor by soaking, biaryl substrates were docked into the structure (Figure 2A). Even though the structure of EX- $\omega$ TA is similar to other fold IV ATAs (see above), we postulate that the interplay of two structural features leads to the ability to convert biaryl ketones: (i) reduced charge and, thus, low polarity

of the active site, and (ii) a methionine at position 47 which probably contributes to position the substrate via S- $\pi$  interactions (Figure 2A).

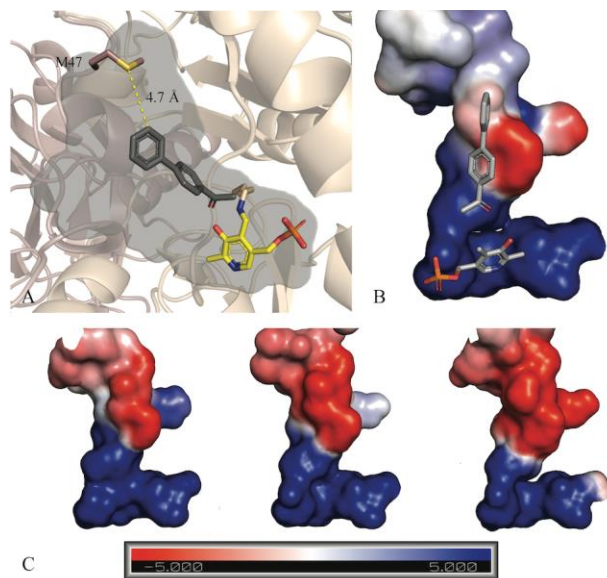


**Figure 2.** Characteristics of EX- $\omega$ TA that enable the conversion of biaryl ketones: (A) M47 helps to position the biaryl ketones (depicted in this Figure is **1a**) via S- $\pi$  interactions; (B) charge of the EX- $\omega$ TA active site (PDB ID: 6FTE) and (C) active site charge of other fold IV ATAs (from left to right): *Aspergillus terreus* AT- $\omega$ TA (PDB ID: 4CE5), *Nectria haematococca*  $\omega$ TA (PDB ID: 4CMD) and *A. fumigatus*  $\omega$ TA (PDB ID: 4CHI). The figures were prepared using the program PyMOL.

Biaryl ketones are hydrophobic and uncharged entities and, thus, bind better in an active site with low polarity. In contrast to other (*R*)-ATAs, which have an active site with high polarity, the EX- $\omega$ TA active site shows a reduced overall charge and is therefore better suited to accommodate the non-polar biaryl moiety of the substrate (compare Figure 2B and C). The methionine at position 47 could also play a key role to enable the conversion of bulky conjugated

substrates: The sulfur of this methionine is located within a distance of 4.7 Å from the outer phenyl-ring and therefore helps to position the biaryl moiety via S- $\pi$  interactions. To confirm this hypothesis, this methionine was replaced by a leucine (as found in *Aspergillus terreus* ATA (AT- $\omega$ TA) and in *A. fumigatus*), and indeed, the conversion of **1a** into **2a** decreased from 83% to 17%.

### Engineering of EX- $\omega$ TA

A consensus design approach was followed to enlarge the small binding pocket of EX- $\omega$ TA for accommodation of larger substituents than the original methyl group. The small binding pocket of EX- $\omega$ TA is defined by the amino acids V60, F113, T273, T274 and A275 (Figure 1A).

Multiple sequence alignment with other ATAs showed that F113 is highly conserved, V60 is rather conserved and also T273, T274 and A275 do not have a lot of variation. If the consecutive amino acids 273 to 275 are taken together as a motif, just four different combinations exist in nature (Figure S2). These are TTA, STA, SSA and SSG. TTA is the combination that takes most space and is the one that is found in EX- $\omega$ TA (and also in the TAs from *A. terreus* and *A. fumigatus*). Hence, the TTA motif was exchanged to STA, SSA and SSG. All variants were soluble and active. EX-STA emerged with significantly improved activity toward all tested substrates except **1a** (Table 1 and Table S4), while the biaryl ethyl ketone **1d** remained unconverted (Table 1, entry 4). Remarkably, EX-STA preserved the exquisite enantioselectivity of the wild type enzyme (>99% *ee*) and the three pyridyl analogues **1h-j** exhibited complete conversion (Table 1, entries 8-10). It seems that this amino acid exchange beneficially impacts the positioning of the substrates in the large binding pocket.

The characterization of EX- $\omega$ TA revealed a quite low thermostability in comparison to other ATAs, especially to AT- $\omega$ TA (Figure S4A). While an incubation at 40°C resulted in a thermal inactivation half-life  $t_{1/2}$  of 11.3 min for EX- $\omega$ TA, no decrease of activity could be observed for AT- $\omega$ TA over the measuring time of 60 min (Figure S4A). To overcome the stability hurdles of EX- $\omega$ TA, stabilizing interactions between amino acid residues were identified within the structure of AT- $\omega$ TA, and consequently introduced into the structure of EX- $\omega$ TA, if they were absent there. To decrease the number of variants but simultaneously increase the chance of success, FoldX<sup>[29]</sup> was used to determine if an amino acid exchange would be likely to increase or decrease the stability. The best resulting variant EX-5 (for other variants see SI) has five amino acid exchanges: K317E introduces a new ionic interaction to R67, and new cation- $\pi$  interactions were created with the amino acid exchanges K110R, L191F and N249F/E300K (Figure S3 and Table S5). K110R interacts with Y320, L191F with R86 and R120. N249F and E300K interact with each other. Indeed, compared to the wild type, the thermal inactivation half-life  $t_{1/2}$  at 45 °C is improved by 10 min and the thermal inactivation  $T_{1/2}$  after 10 min increased by 4.4 °C (Figure 3 and Table 2). This thermostable variant EX-5 retained the same excellent enantioselectivity as the wild type (>99% *ee* in all cases). Interestingly, however, the substrate tolerance showed significant differences: for example, EX-5 poorly converted **1a** (15%, Table 1, entry 1) but was very active toward the fluorine-substituted derivative **1e** (84% Table 1, entry 5)

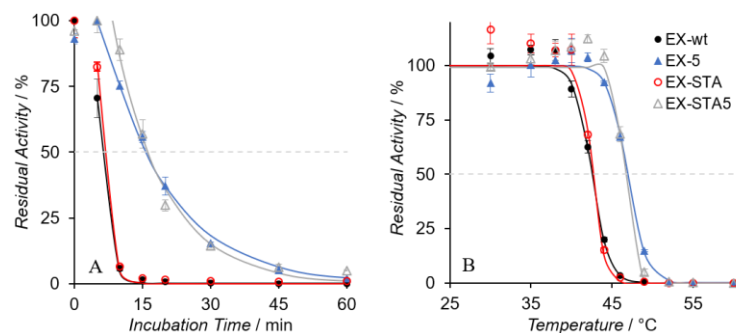


**Figure 3.** Thermal inactivation properties of wild type EX- $\omega$ TA and variants thereof. (A)

Thermal inactivation half-life  $t_{1/2}$  at 45°C. (B) Thermal inactivation at different temperatures

$T_{1/2}^{10}$ . Error bars are the mean SD values of three samples. Solid lines represent the fitted data.

**Table 2.** Stability constants of wild-type EX- $\omega$ TA and variants thereof.

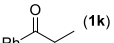
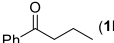
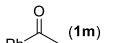
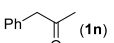
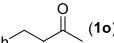
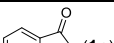
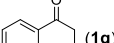
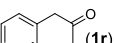
	EX-wt	EX-STA	EX-5	EX-STA5
$\Delta\Delta G_{\text{fold}}$ [kcal/mol]	-	-0.92	-3.03	-4.06
$\Delta\Delta G_{\text{binding}}$ [kcal/mol]	-	0	-0.26	-0.21
$T_{1/2}^{10 \text{ min}}$ [°C]	42.5	42.6	46.9	46.1
$\Delta T_{1/2}^{10 \text{ min}}$ [°C]	-	0.1	4.4	3.6
$t_{1/2}^{45^\circ\text{C}}$ [min]	5.6	5.9	15.8	16.3
$\Delta t_{1/2}^{45^\circ\text{C}}$ [min]	-	0.3	10.2	10.7

Since EX-STA converted most of the substrates more efficiently than the wild type (TTA) or EX-SSA and EX-SSG (Table S4), the STA motif was combined with the amino acid exchanges from the more thermostable variant EX-5. As a result, the combined variant EX-STA5 now encompasses similar or only slightly lower activity than EX-STA (Table 1) but also shows an improved stability like EX-5 (Table 2 and Figure 3). These results reveal that the acquisition of the enhanced enzymatic activity did not have a detrimental effect on stability, which makes the resulting ATA EX-STA5 a more robust biocatalyst for its implementation in an industrial setting.

### Substrate Scope of EX- $\omega$ TA and its Variants Toward Non-Biaryl Ketones

Once the transamination of biaryl ketones was established employing either EX- $\omega$ TA or its variants, we sought to deepen the knowledge about the structural requirements of these new ATAs. Thus, a series of non biaryl ketones was assayed with the EX-wildtype and the three best variants (Table 3).

**Table 3.** Substrate scope of EX- $\omega$ TA and its variants toward non-biaryl ketones.<sup>[a]</sup>

Entry	Substrate	Conversion (%)				<i>ee</i> (%) <sup>[b]</sup>
		EX-wt	EX-STA	EX-STA5	EX-5	
1	 (1k)	<5	7	<5	<5	n.d. <sup>[c]</sup>
2	 (1l)	-	-	-	-	-
3	 (1m)	15	60	15	60	>99
4	 (1n)	95	76	55	65	>99
5	 (1o)	67	66	62	60	>99
6	 (1p)	-	<5	<5	-	n.d. <sup>[c]</sup>
7	 (1q)	-	-	-	-	-
8	 (1r)	49	94	93	52	>99

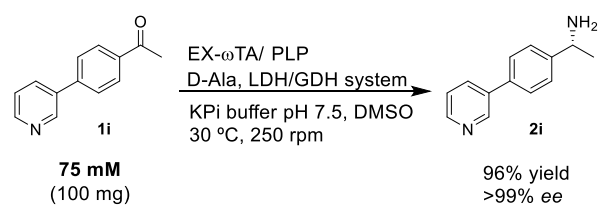
[a] Reaction conditions: 20 mM ketone dissolved in DMSO (5% v/v), 100 mM potassium phosphate buffer, pH 7.5, 1 mM PLP, 0.1 mM NAD<sup>+</sup>, 20 U ATA, 130 mM D-alanine, 60 mM glucose, 30 U GDH and 90 U LDH, shaken for 24 h at 250 rpm and 30 °C. Conversions were measured by HPLC. [b] Measured by chiral HPLC; the *ee* is the same for all four enzymes and the (*R*)-configuration was obtained in all cases. [c] Not detected due to low activity.

As expected, conversions of propiophenone (**1k**) stayed rather low and none of the ATAs was capable to convert 1-phenylbutan-2-one (**1l**) which confirms the size restrictions of the small binding pocket pointed out before (Table 3, entries 1-2). In contrast, different methyl monoaryl ketones such as acetophenone (**1m**), 1-phenylpropan-2-one (**1n**) and 4-phenylbutan-2-one (**1o**) with variable length of the alkyl chain exhibited moderate to good conversions depending on the ATA variant and ketone considered (Table 3, entries 3-6). Further extension to benzo-fused cyclic ketones revealed that those with the carbonyl moiety contiguous to the methylene bridge were unreactive (**1p-q**, Table 3, entries 6-7). However, 2-tetralone (**1r**) afforded excellent conversions catalyzed by both EX-STA and EX-STA5 (Table 3, entry 8).

### Preparative-scale Biaryl Amine Synthesis

Taking the EX-STA-catalyzed transamination of **1i** as a model reaction (Table 1, entry 9), several process parameters were investigated on an analytical scale. In detail, the formulation of the biocatalyst, the amino donor, the concentration of substrate and the enzyme loading were assessed. Importantly, the variants EX-5, EX-STA and EX-STA5 retained their activity as a lyophilized powder of the lysate in contrast to the wild type enzyme (Figure S5). In addition, the variants also accepted isopropylamine as an amino donor (Figure S6) although with lower conversions than those measured with alanine. By using EX-STA as a lyophilized powder the upper limit for the substrate concentration was established at 75 mM (Figure S7). Finally, the enzyme loading was optimized to 3.2 U/mg of substrate (Figure S8).

To illustrate the synthetic applicability of the new ATAs, a preparative-scale biotransformation was carried out. The target biotransformation was accomplished at 100 mg-scale and 75 mM of **1i** to afford enantiopure (*R*)-**2i** in excellent isolated yield (96%) after extractive work up and without need for further purification (Scheme 2).



**Scheme 2.** Preparative-scale transamination of **1i** catalyzed by EX- $\omega$ TA.

## CONCLUSION

In summary, we report a new (*R*)-selective ATA which naturally converts biaryl ketones to the corresponding enantiomerically pure amines. With the help of its crystal structure, structural features were identified which could explain its unique ability. The activity and stability of this new ATA was further improved by protein engineering, resulting in improved biocatalysts whose applicability was illustrated through a preparative-scale example. Our results highlight the value of nature's biodiversity and extreme environments as an ever-increasing source of new genomes and metagenomes to identify unprecedented catalytic activities which can lead to novel industrially robust biocatalysts.

## ASSOCIATED CONTENT

### Supporting Information.

Supporting Tables: conserved motifs of fold IV PLP-dependent enzymes, list of primers, protein crystallography data;

Additional experimental procedures and data for protein engineering;

Supporting Figures: omit electron density of PLP in the structure, biocatalyst formulation study, transamination of **1i** using isopropylamine as amino donor, substrate loading studies, enzyme loading studies;



Detailed results of enzymatic transamination of ketones **1a-j**; assignments of the absolute configurations, spectroscopic data of amines **2a-b, e-j**; HPLC analytical data; copies of chiral-HPLC chromatograms; copies of NMR spectra

This information is available free of charge on ACS Publications website.

## **AUTHOR INFORMATION**

### **Corresponding Author**

\* Email: kerstin.steiner11@googlemail.com

### **Author Contributions**

The manuscript was written through contributions of all authors. All authors have given approval to the final version of the manuscript.

### **Funding Sources**

The Biocascades project is supported by the European Commission under the Horizon 2020 program through the Marie Skłodowska-Curie actions: ITN-EID under the Environment Cluster (Grant Number 634200).

### **Notes**

The authors declare no competing financial interest.

## **ACKNOWLEDGMENT**

The Biocascades project is supported by the European Commission under the Horizon 2020 program through the Marie Skłodowska-Curie actions: ITN-EID under the Environment Cluster (Grant Number 634200). We thank Math Boesten for assistance with HPLC analysis.

## REFERENCES

- (1) Jarvis, L. M. The year in new drugs. *Chem. Eng. News* 2016, 94, 12–17.
- (2) Kelly, S. A.; Pohle, S.; Wharry, S.; Mix, S.; Allen, C. C. R.; Moody, T. S.; Gilmore, B. F. Application of  $\omega$ -Transaminases in the Pharmaceutical Industry. *Chem. Rev.* 2018, 118, 349–367.
- (3) Malik, M. S.; Park, E. S.; Shin, J. S. Features and technical applications of  $\omega$ -transaminases. *Appl. Microbiol. Biotechnol.* 2012, 94, 1163–1171.
- (4) Höhne, M.; Schätzle, S.; Jochens, H.; Robins, K.; Bornscheuer, U. T. Rational assignment of key motifs for function guides *in silico* enzyme identification. *Nat. Chem. Biol.* 2010, 6, 807–813.
- (5) (a) Dourado, D. F. A. R.; Pohle, S.; Carvalho, A. T. P.; Dheeman, D. S.; Caswell, J. M.; Skvortsov, T.; Miskelly, I.; Brown, R. T.; Quinn, D. J.; Allen, C. C. R.; Kulakov, L.; Huang, M.; Moody, T. S. Rational Design of a (*S*)-Selective-Transaminase for Asymmetric Synthesis of (1*S*)-1-(1,1'-biphenyl-2-yl)ethanamine. *ACS Catal.* 2016, 6, 7749–7759; (b) Pavlidis, I. V.; Weiß, M. S.; Genz, M.; Spurr, P.; Hanlon, S. P.; Wirz, B.; Iding, H.; Bornscheuer, U. T. Identification of (*S*)-selective transaminases for the asymmetric synthesis of bulky chiral amines. *Nat. Chem.* 2016, 8, 1–7; (c) Han, S. W.; Park, E. S.; Dong, J. Y.; Shin, J. S. Mechanism-Guided Engineering of  $\omega$ -Transaminase to Accelerate Reductive Amination of Ketones. *Adv. Synth. Catal.* 2015, 357, 1732–1740; (d) Weiß, M. S.; Pavlidis, I. V.; Spurr, P.; Hanlon, S. P.; Wirz, B.; Iding, H.; Bornscheuer, U. T. Amine transaminase engineering for spatially bulky substrate acceptance. *ChemBioChem* 2017, 18, 1022–1026; (e) Weiß, M. S.; Pavlidis, I. V.; Spurr, P.; Hanlon, S. P.; Wirz, B.; Iding, H.; Bornscheuer, U. T. Protein-engineering of an amine transaminase for the stereoselective synthesis of a pharmaceutically

- relevant bicyclic amine. *Org. Biomol. Chem.* 2016, 14, 10249–10254; (f) Nobili, A.; Steffen-Munsberg, F.; Kohls, H.; Trentin, I.; Schulzke, C.; Höhne, M.; Bornscheuer, U. T. Engineering the Active Site of the Amine Transaminase from *Vibrio fluvialis* for the Asymmetric Synthesis of Aryl– Alkyl Amines and Amino Alcohols. *ChemCatChem* 2015, 7, 757–760.
- (6) Calvelage, S.; Dörr, M.; Höhne, M.; Bornscheuer, U. T. A Systematic Analysis of the Substrate Scope of (*S*)- and (*R*)-selective Amine Transaminases. *Adv. Synth. Catal.* 2017, 359, 4235-4243.
- (7) Savile, C. K.; Janey, J. M.; Mundorff, E. C.; Moore, J. C.; Tam, S.; Jarvis, W. R.; Colbeck, J. C.; Krebber, A.; Fleitz, F. J.; Brands, J.; Devine, P. N.; Huisman, G. W.; Hughes, G. J. Biocatalytic Asymmetric Synthesis of Chiral Amines from Ketones Applied to Sitagliptin Manufacture. *Science* 2010, 329, 305–309.
- (8) (a) Horton, D. A.; Bourne, G. T.; Smythe, M. L. The Combinatorial Synthesis of Bicyclic Privileged Structures or Privileged Substructures. *Chem. Rev.* 2003, 103, 893–930; (b) Yet, L. Biaryls in *Privileged Structures in Drug Discovery: Medicinal Chemistry and Synthesis*, John Wiley & Son, Hoboken, NJ, USA, 2018. P. 83-154
- (9) Dawood, A. W. D.; Bassut, J.; de Souza, R. O. M. A.; Bornscheuer, U. T. Combination of the Suzuki–Miyaura Cross-Coupling Reaction with Engineered Transaminases. *Chem. Eur. J.* 2018, 16009-16013.
- (10) (a) Sayer, C.; Martinez-Torres, R. J.; Richter, N.; Isupov, M. N.; Hailes, H. C.; Littlechild, J. A.; Ward, J. M. The substrate specificity, enantioselectivity and structure of the (*R*)-selective amine:pyruvate transaminase from *Nectria haematococca*. *FEBS J.* 2014, 281, 2240–2253; (b) Thomsen, M.; Skalden, L.; Palm, G. J.; Höhne, M.; Bornscheuer, U. T.;

- Hinrichs, W. Crystallographic characterization of the (*R*)-selective amine transaminase from *Aspergillus fumigatus*. *Acta Crystallogr. Sect. D Biol. Crystallogr.* 2014, 70, 1086–1093; (c) Schätzle, S.; Steffen-Munsberg, F.; Thontowi, A.; Höhne, M.; Robins, K.; Bornscheuer, U. T. Enzymatic Asymmetric Synthesis of Enantiomerically Pure Aliphatic, Aromatic and Arylaliphatic Amines with (*R*)-Selective Amine Transaminases. *Adv. Synth. Catal.* 2011, 353, 2439–2445; (d) Jiang, J.; Chen, X.; Zhang, D.; Wu, Q.; Zhu, D. Characterization of (*R*)-selective amine transaminases identified by in silico motif sequence blast. *Appl. Microbiol. Biotechnol.* 2015, 99, 2613–2621; (e) Łyskowski, A.; Gruber, C.; Steinkellner, G.; Schürmann, M.; Schwab, H.; Gruber, K.; Steiner, K. Crystal Structure of an (*R*)-Selective  $\omega$ -Transaminase from *Aspergillus terreus*. *PLoS One* 2014, 9, e87350. (f) Guan, L. J.; Ohtsuka, J.; Okai, M.; Miyakawa, T.; Mase, T.; Zhi, Y.; Hou, F.; Ito, N.; Iwasaki, A.; Yasohara, Y.; Tanokura, M. A new target region for changing the substrate specificity of amine transaminases. *Sci. Rep.* 2015, 5, 10753.
- (11) Altschul, S. F.; Gish, W.; Miller, W.; Myers, E. W.; Lipman, D. J. Basic local alignment search tool. *J. Mol. Biol.* 1990, 215, 403–410.
- (12) Tamura, K.; Stecher, G.; Peterson, D.; Filipski, A.; Kumar, S. MEGA6: Molecular Evolutionary Genetics Analysis Version 6.0. *Mol. Biol. Evol.* 2013, 30, 2725–9.
- (13) De Hoog, G. S.; Zeng, J. S.; Harrak, M. J.; Sutton, D. A. *Exophiala xenobiotica* sp. nov., an opportunistic black yeast inhabiting environments rich in hydrocarbons. *Antonie van Leeuwenhoek, Int. J. Gen. Mol. Microbiol.* 2006, 90, 257–268.
- (14) Balzer, D.; Ziegelin, G.; Pansegrau, W.; Kruff, V.; Lanka, E. KorB protein of promiscuous plasmid RP4 recognizes inverted sequence repetitions in regions essential for conjugative plasmid transfer. *Nucleic Acids Res.* 1992, 20, 1851–8.

- (15) Gasteiger, E.; Hoogland, C.; Gattiker, A.; Duvaud, S.; Wilkins, M. R.; Appel, R. D.; Bairoch, A. Protein Identification and Analysis Tools on the ExPASy Server. *Proteomics Protoc. Handb.* 2005, 571–607.
- (16) Kabsch, W. XDS. *Acta Crystallogr. D. Biol. Crystallogr.* 2010, 66, 125–32.
- (17) McCoy, A. J.; Grosse-Kunstleve, R. W.; Adams, P. D.; Winn, M. D.; Storoni, L. C.; Read, R. J. Phaser crystallographic software. *J. Appl. Crystallogr.* 2007, 40, 658–674.
- (18) Emsley, P.; Lohkamp, B.; Scott, W. G.; Cowtan, K. Features and development of Coot. *Acta Crystallogr. Sect. D Biol. Crystallogr.* 2010, 66, 486–501.
- (19) Murshudov, G. N.; Skubák, P.; Lebedev, A. A.; Pannu, N. S.; Steiner, R. A.; Nicholls, R. A.; Winn, F. Long, M. D.; Vagin, A. A. REFMAC5 for the refinement of macromolecular crystal structures. *Acta Crystallogr. Sect. D Biol. Crystallogr.* 2011, 67, 355–367.
- (20) (a) Chen, V. B.; Arendall, W. B.; Headd, J. J.; Keedy, D. A.; Immormino, R. M.; Kapral, G. J.; Murray, L. W.; Richardson, J. S.; Richardson, D. C. MolProbity: all-atom structure validation for macromolecular crystallography. *Acta Crystallogr. Sect. D Biol. Crystallogr.* 2010, 66, 12–21. (b) Williams, C. J.; Headd, J. J.; Moriarty, N. W.; Prisant, M. G.; Videau, L. L.; Deis, L. N.; Verma, V.; Keedy, D. A.; Hintze, B. J.; Chen, V. B.; Jain S.; Lewis, S. M.; Arendall, W. B.; Snoeyink, J.; Adams, P. D.; Lovell, S. C.; Richardson, J. S.; Richardson, D. C. MolProbity: More and better reference data for improved all-atom structure validation. *Protein Sci.* 2017, 27, 293–315.
- (21) Krissinel, E.; Henrick K. Inference of Macromolecular Assemblies from Crystalline State. *J. Mol. Biol.* 2007, 372, 774–79.

- (22) Schätzle, S.; Höhne, M.; Redestad, E.; Robins, K.; Bornscheuer, U. T. Rapid and Sensitive Kinetic Assay for Characterization of  $\omega$ -Transaminases. *Anal. Chem.* 2009, 81, 8244–8248.
- (23) Smith, D. L.; Budgen, N.; Bungard, S. J.; Danson, M. J.; Hough, D. W. Purification and characterization of glucose dehydrogenase from the thermoacidophilic archaeobacterium *Thermoplasma acidophilum*. *Biochem. J.* 1989, 261, 973-977.
- (24) Kosjek, B.; Stampfer, W.; Pogorevc, M.; Goessler, W.; Faber, K.; Kroutil, W. Purification and characterization of a chemotolerant alcohol dehydrogenase applicable to coupled redox reactions. *Biotechnol. Bioeng.* 2004, 86, 55-62.
- (25) Paris, J.; Ríos-Lombardía, N.; Morís, F.; Gröger, H.; González-Sabín, J. Novel Insights into the Combination of Metal- and Biocatalysis: Cascade One-Pot Synthesis of Enantiomerically Pure Biaryl Alcohols in Deep Eutectic Solvents. *ChemCatChem* 2018, 10, 4417-4423.
- (26) Fulmer, G. R.; Miller, A. J. M.; Sherden, N. H.; Gottlieb, H. E.; Nudelman, A.; Stoltz, B. M.; Bercaw, J. E.; Goldberg, K. I. NMR Chemical Shifts of Trace Impurities: Common Laboratory Solvents, Organics, and Gases in Deuterated Solvents Relevant to the Organometallic Chemist. *Organometallics* 2010, 29, 2176-2179.
- (27) (a) Dawood, A. W. H.; Weiß, M. S.; Schulz, C.; Pavlidis, I. V.; Iding, H.; de Souza, R. O. M. A.; Bornscheuer, U. T. Isopropylamine as Amine Donor in Transaminase-Catalyzed Reactions: Better Acceptance through Reaction and Enzyme Engineering. *ChemCatChem* 2018, 10, 3943-3949. (b) Kelefiotis-Stratidakis, P.; Tyrikos-Ergas, T.; Pavlidis, I. V. The challenge of using isopropylamine as an amine donor in transaminase catalysed reactions. *Org. Biomol. Chem.* 2018. doi:10.1039/c8ob02342e.

- (28) Holm, L.; Rosenström, P. Dali server: conservation mapping in 3D. *Nucleic Acids Res.* 2010, 38, W545-W549.
- (29) van Durme, J.; Delgado, J.; Stricher, F.; Serrano, L.; Schymkowitz, J.; Rousseau, F. A graphical interface for the FoldX forcefield. *Bioinformatics* 2011, 27, 1711–1712.

TOC graphic

